Electronic Supplementary Material (ESI) for RSC Advances
This journal is © The Royal Society of Chemistry 2022

Electronic Supplementary Information

Colorimetric screening of elevated urinary mercury levels by a novel Hg^{2+}-selective probe of resorufin phosphinothioate

Myung Gil Choi, Byung Hoon Yun, Hyeong Min Kim, Sangdoo Ahn,* Suk-Kyu Chang*

Department of Chemistry, Chung-Ang University, Seoul 06974, Republic of Korea

Contents

signaling of **MP-1** expressed by absorbance ratio (A_{576}/A_{457}).

Fig. S11. Calibration curve of Hg^{2+} analysis in artificial urine by probe **MP-1** as plotted by absorbance ratio (A_{576}/A_{457}).

Fig. S12. Calibration curve expressed by color channel levels of image for Hg^{2+} signaling in artificial urine.

Fig. S13. ^{1}H NMR spectrum of **MP-1** in DMSO-d_6 (600 MHz).

Fig. S14. ^{13}C NMR spectrum of **MP-1** in DMSO-d_6 (150 MHz).

Fig. S15. High-resolution FAB mass spectrum of **MP-1**.

Experimental details

1. General

Resorufin sodium salt was procured from Merck KGaA. Dimethylthiophosphinoyl chloride (97.0%) was obtained from TCI. Artificial urine (Sigmatrix Urine Diluent) was purchased from Merck KGaA. Other chemicals (metal salts (97% ~ 99%) and spectroscopic grade solvents (DMF: 99.8%, dichloromethane: 99.8%, acetonitrile: 99.9%) were obtained from Merck KGaA. UV–vis and fluorescence spectra were acquired using Scinco S-3100 and FS-2 spectrophotometers, respectively. High-resolution mass spectrometry (HRMS) data with fast atom bombardment (FAB) ionization were collected using a JEOL JMS-700 mass spectrometer. High-performance liquid chromatography (HPLC) experiments were performed with a Yong In YL9100 Plus HPLC System. Column chromatography was carried out using silica gel (Merck, 240 mesh).

2. Estimation of detection limit

The Hg^{2+} detection limit was estimated following the IUPAC guidelines ($3s_{blk}/m$) using a UV–vis spectrophotometer, where s_{blk} is the standard deviation of the absorbance ratio at 576 and 457 nm (A_{576}/A_{457}) of the probe solution (5.0 μM, n = 12) and m is the slope of the titration plot.[S1]

Table. S1. Summary of the optical urinary mercury sensing systems

Material	Condition	Signal	Interference tested	Dilution ratio[a]	Detection limit (nM)	Ref
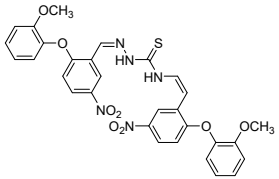	HEPES buffer (3 mM) /acetonitrile (99:1, *v/v*)	Colorimetry	Metal ions	0.003	27	S2
DNA-Gold nanoparticles	pH 7.5 phosphate buffer	Colorimetry	Metal ions	0.1	0.01	S3
DNA-Gold nanoclusters	pH 6.0 phosphate buffer	Fluorescence	Metal ions	0.3	83	S4
Carbon dots	aqueous solutions	Fluorescence	Metal ions	-	201	S5
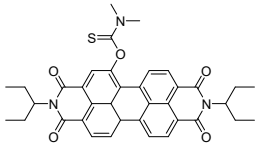	90 % HEPES buffer /DMSO (9:1, *v/v*)	Colorimetry and Fluorescence	Metal ions	0.1	7.4	S6
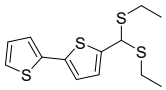	aqueous solution	Fluorescence	Metal ions	0.01	19	S7
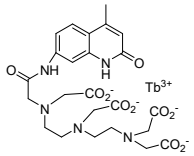	aqueous solution with neutral pH	Fluorescence	Metal ions	0.01	0.8	S8
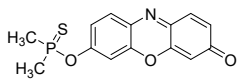	pH 7.4 PBS with 20% acetonitrile	Colorimetry and Fluorescence	Metal ions and anions	0.5	12	This work

[a] A dilution ratio is the ratio of the volume of urine solution in a total volume of a measuring sample.

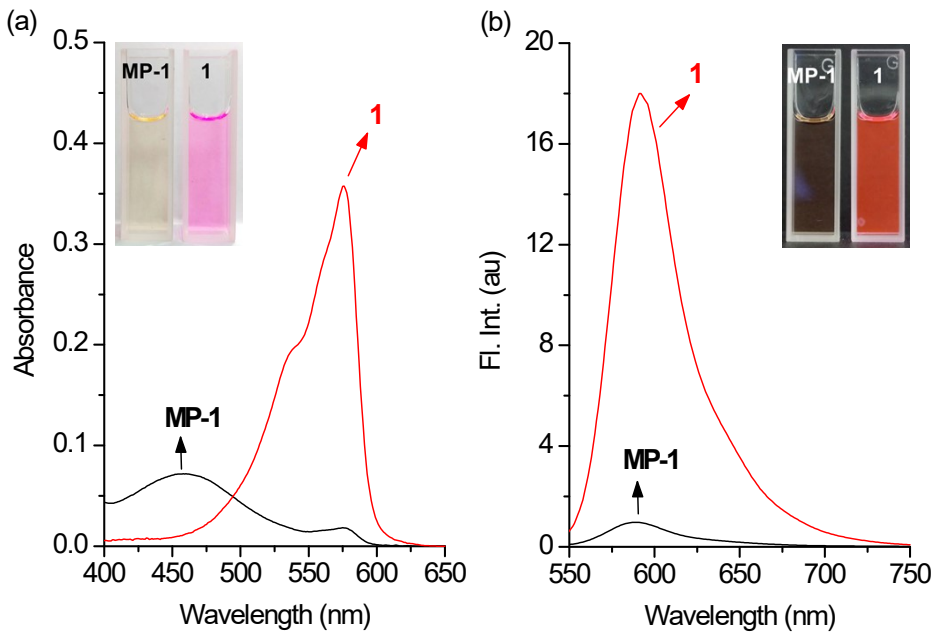

Fig. S1. (a) UV–vis and (b) fluorescence spectra of **MP-1** and its Hg^{2+} signaling product **1**. [**MP-1**] = [**1**] = 5.0 μM, [citrate] = 5.0 mM, [PBS 7.4] = 10 mM in aqueous solution containing 20% (*v*/*v*) acetonitrile. For (b), λ_{ex} = 492 nm.

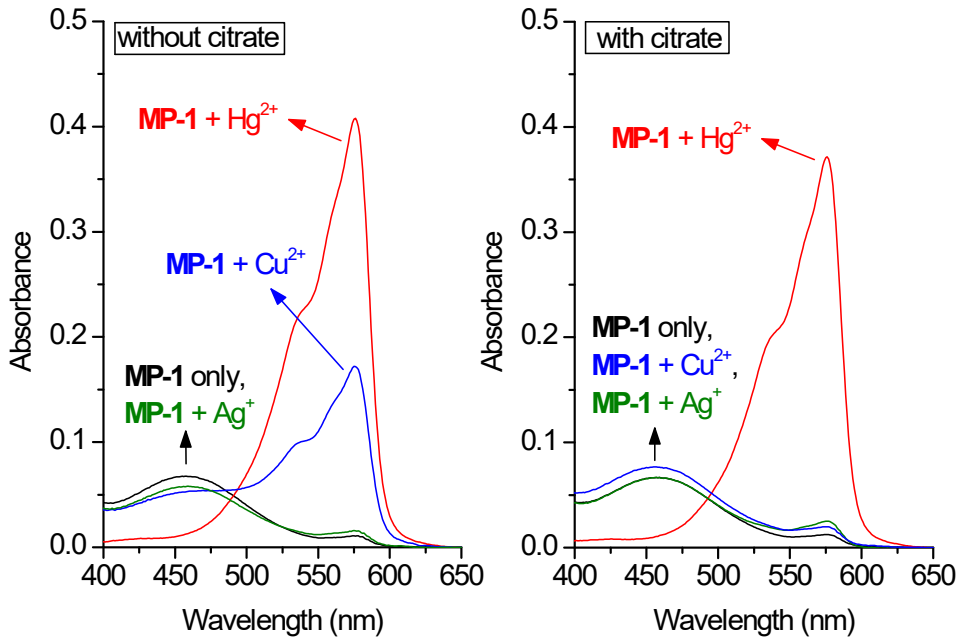

Fig. S2. UV–vis spectra of **MP-1** in the presence of thiophilic metal ions with or without citrate as metal ion scavenger. [**MP-1**] = 5.0 μM, [M^{n+}] = 100 μM, [citrate] = 5.0 mM, [PBS 7.4] = 10 mM in aqueous solution containing 20% (*v*/*v*) acetonitrile.

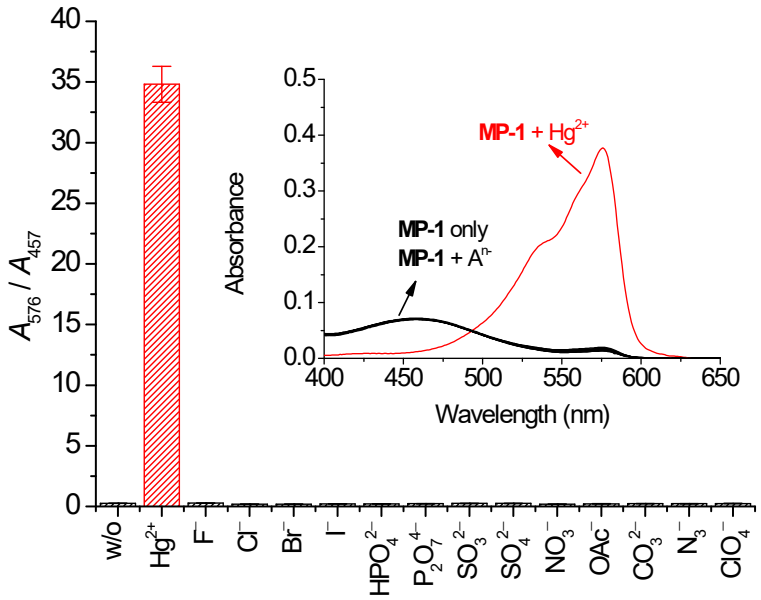

Fig. S3. Changes in absorbance ratio (A_{576}/A_{457}) of **MP-1** in the presence of common anions. [**MP-1**] = 5.0 μM, [Hg^{2+}] = [A^{n-}] = 100 μM, [citrate] = 5.0 mM, [PBS 7.4] = 10 mM in aqueous solution containing 20% (*v*/*v*) acetonitrile. Number of measurements (*n*) = 3.

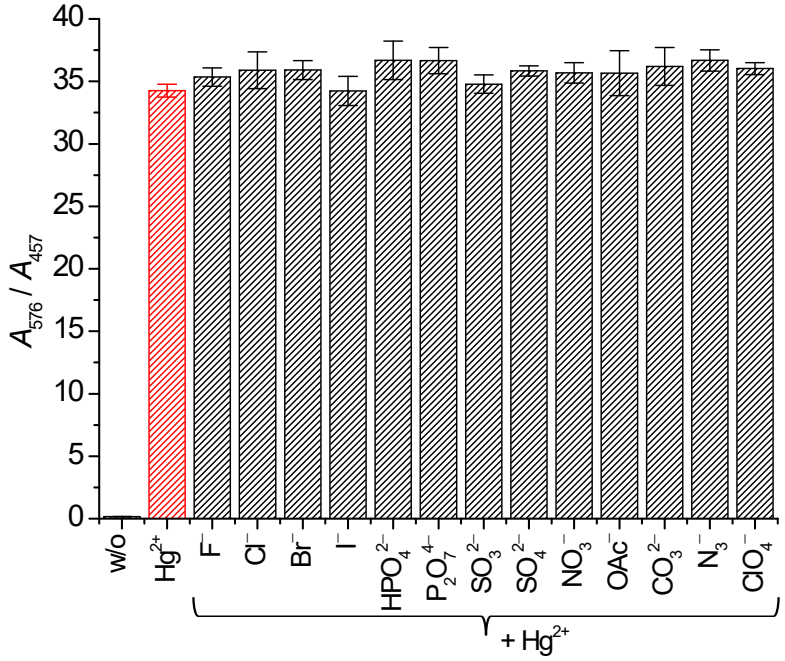

Fig. S4. Changes in absorbance ratio (A_{576}/A_{457}) of Hg^{2+} signaling by **MP-1** in the presence of common anions as background. [**MP-1**] = 5.0 μM, [Hg^{2+}] = [A^{n-}] = 100 μM, [citrate] = 5.0 mM, [PBS 7.4] = 10 mM in aqueous solution containing 20% (*v*/*v*) acetonitrile. Number of measurements (*n*) = 3.

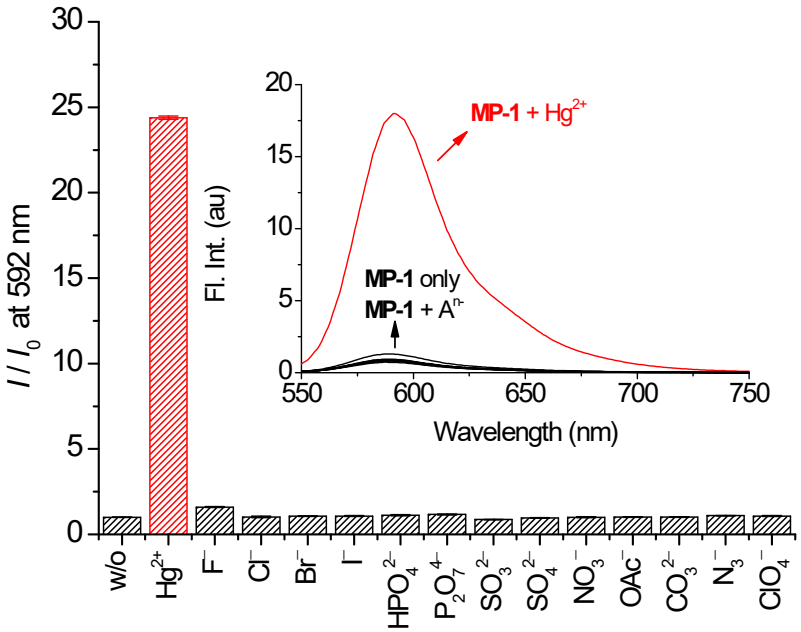

Fig. S5. Changes in fluorescence intensity at 592 nm of **MP-1** as plotted by intensity ratio I/I_0 in the presence of common anions. [**MP-1**] = 5.0 μM, [Hg^{2+}] = [A^{n-}] = 100 μM, [citrate] = 5.0 mM, [PBS 7.4] = 10 mM in aqueous solution containing 20% (*v*/*v*) acetonitrile. λ_{ex} = 492 nm. Number of measurements (*n*) = 3.

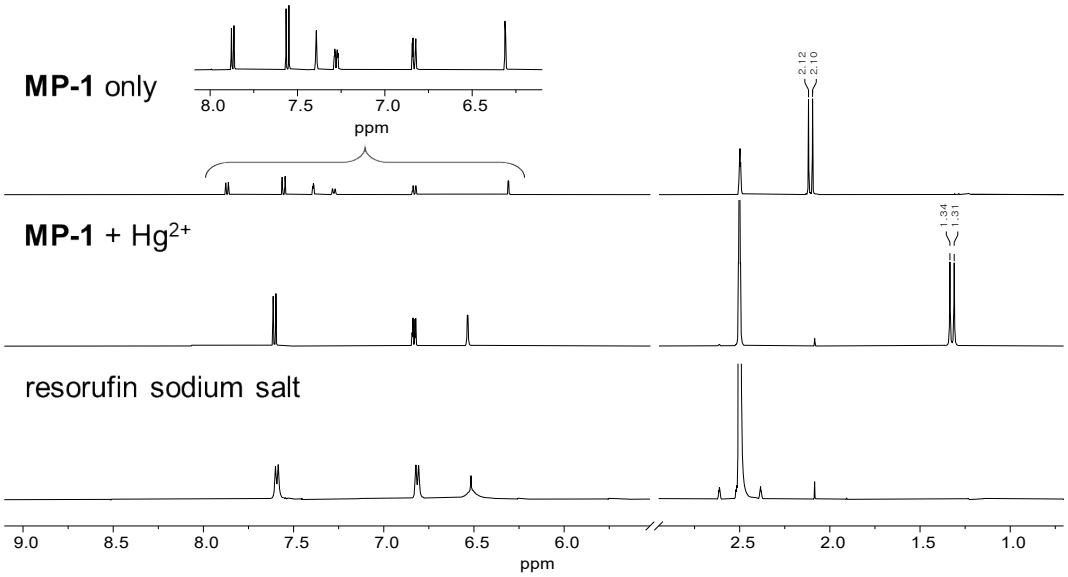

Fig. S6. ^{1}H NMR spectrum of (a) **MP-1**, (b) **MP-1** + Hg^{2+}, and (c) resorufin sodium salt in DMSO-d_6. [**MP-1**] = [resorufin sodium salt] = 5.0 mM. For (b), the spectrum (**MP-1** + Hg^{2+}) was obtained using a mixture of **MP-1** (5.0 mM) and $Hg(ClO_4)_2$ (10.0 mM) in DMSO-d_6.

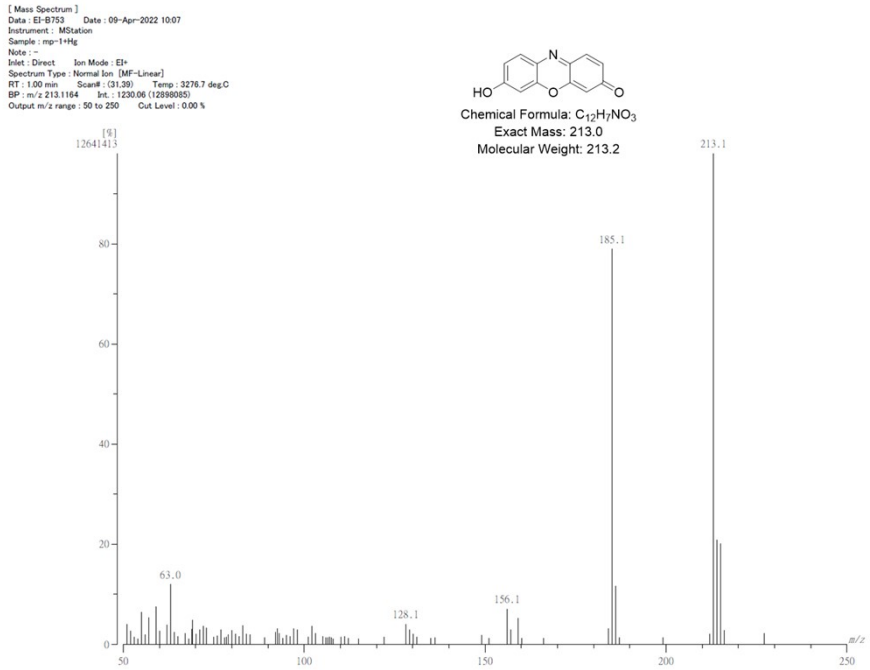

Fig. S7. EI mass spectrum for the Hg^{2+} signaling product of **MP-1**.

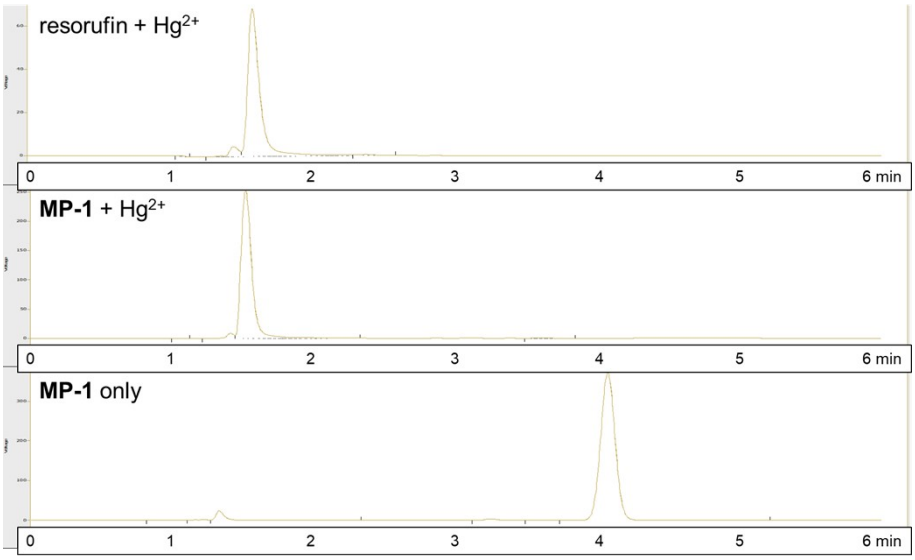

Fig. S8. HPLC evidence of Hg^{2+} signaling by **MP-1**. The middle chromatogram (**MP-1** + Hg^{2+}) was obtained for the signaling reaction product (condition: [**MP-1**] = 5.0 μM, [Hg^{2+}] = 100 μM, [citrate] = 5.0 mM, [PBS 7.4] = 10 mM in aqueous solution containing 20% (*v/v*) acetonitrile). Eluent: 50% aq. acetonitrile, column: reversed phase column C18 (Sunfire, 4.6×150 mm), flow rate = 1.0 mL/min.

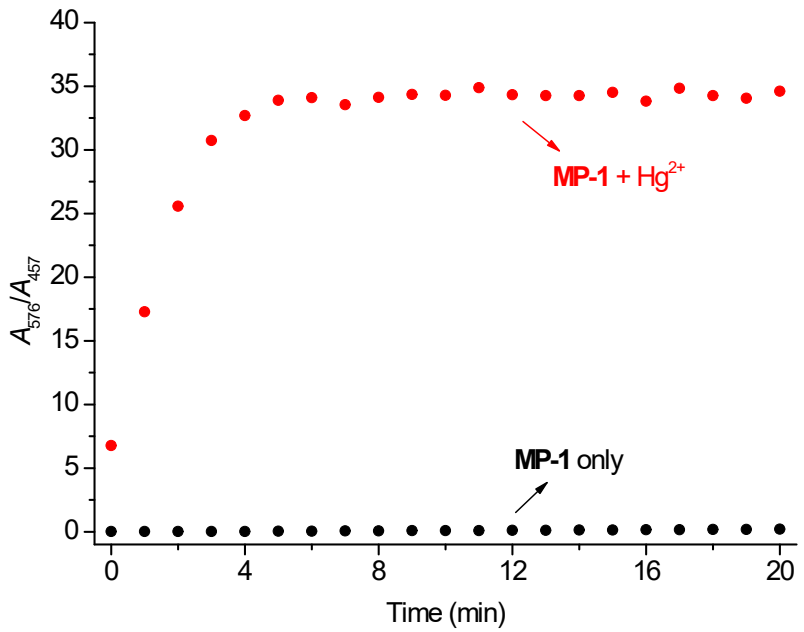

Fig. S9. Time-dependent Hg^{2+} signaling of **MP-1** plotted by change in absorbance ratio (A_{576}/A_{457}). [**MP-1**] = 5.0 μM, [Hg^{2+}] = 100 μM, [citrate] = 5.0 mM, [PBS 7.4] = 10 mM in aqueous solution containing 20% (*v*/*v*) acetonitrile.

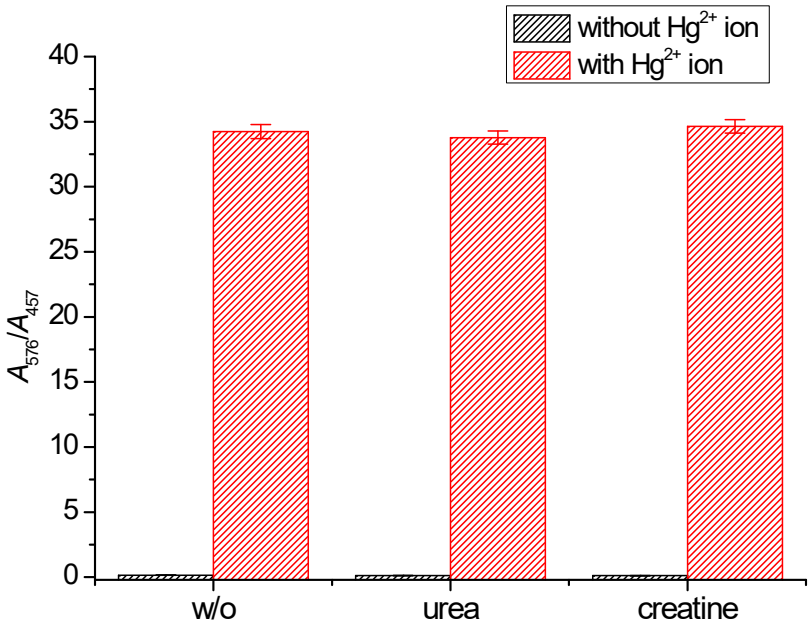

Fig. S10. Effects of representative urine components urea and creatine on Hg^{2+} signaling of **MP-1** expressed by absorbance ratio (A_{576}/A_{457}). [**MP-1**] = 5.0 μM, [Hg^{2+}] = 100.0 μM, [urea] = 178 mM, [creatine] = 7.6 mM, [citrate] = 5.0 mM, [PBS 7.4] = 10 mM in aqueous solution containing 20% (*v*/*v*) acetonitrile. Number of measurements (*n*) = 3.

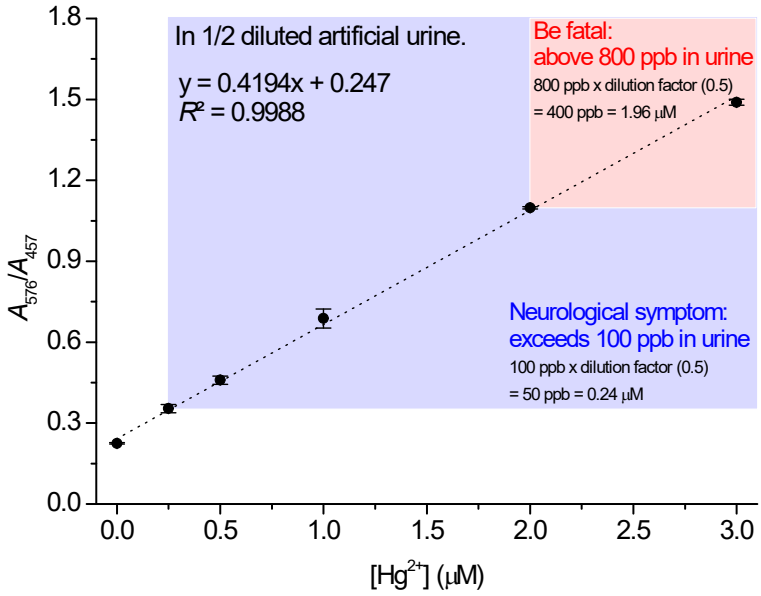

Fig. S11. Calibration curve of Hg^{2+} analysis in artificial urine by probe **MP-1** as plotted by absorbance ratio (A_{576}/A_{457}). [**MP-1**] = 5.0 μM, [Hg^{2+}] = 0–3.0 μM, [citrate] = 5.0 mM, [PBS 7.4] = 10 mM in aqueous solution containing 20% (*v*/*v*) acetonitrile. The regions marked in blue and red indicate the neurological symptom and fatal zones, respectively. Number of measurements (*n*) = 3.

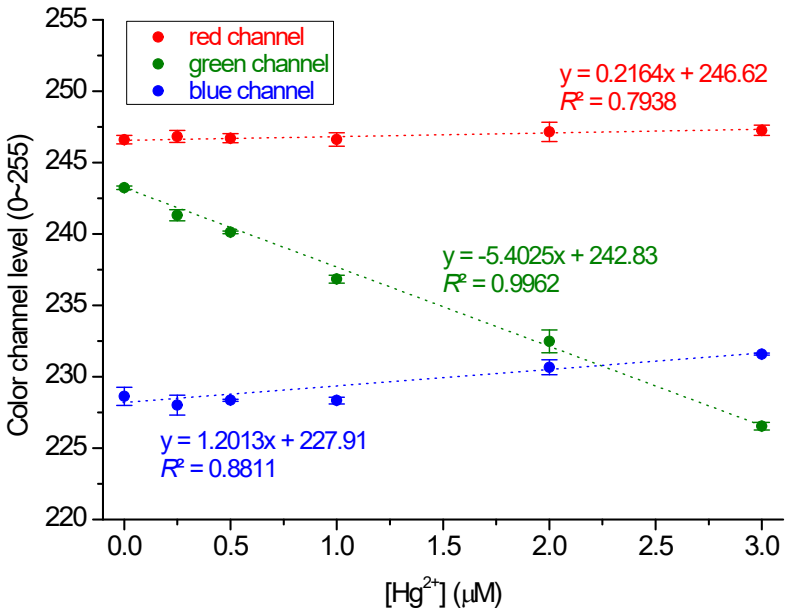

Fig. S12. Calibration curve expressed by color channel levels of image for Hg^{2+} signaling in artificial urine. [**MP-1**] = 5.0 μM, [Hg^{2+}] = 0–3.0 μM, [citrate] = 5.0 mM, [PBS 7.4] = 10 mM in aqueous solution containing 20% (*v*/*v*) acetonitrile. Number of measurements (*n*) = 3.

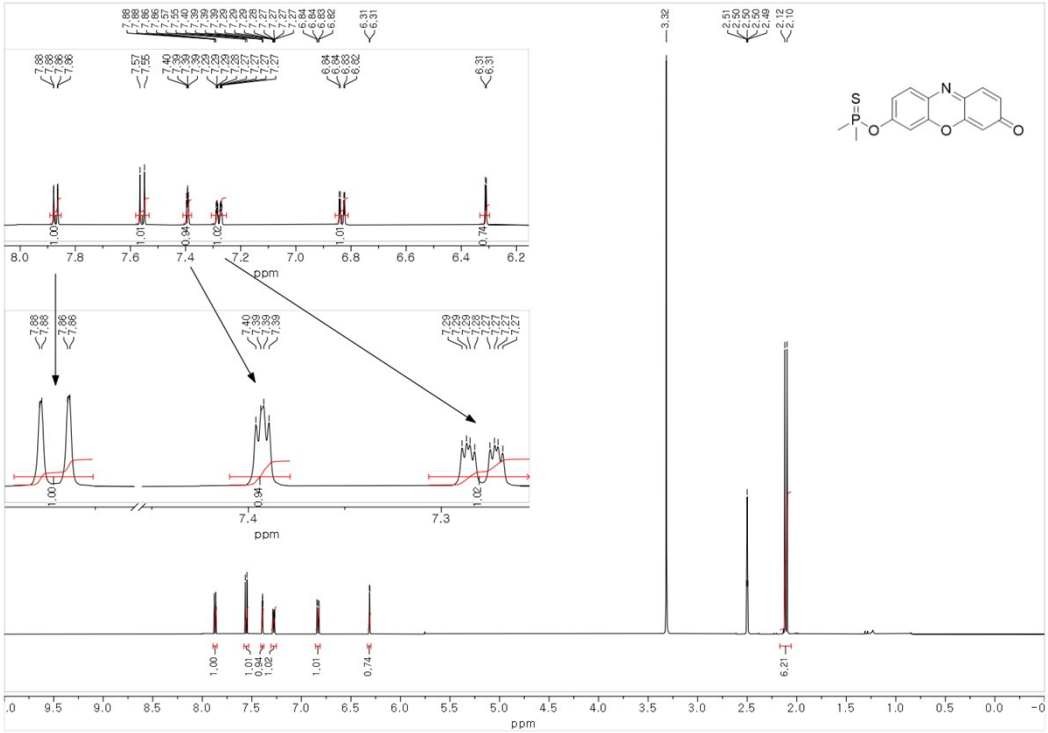

Fig. S13. ^{1}H NMR spectrum of **MP-1** in DMSO-d_6 (600 MHz).

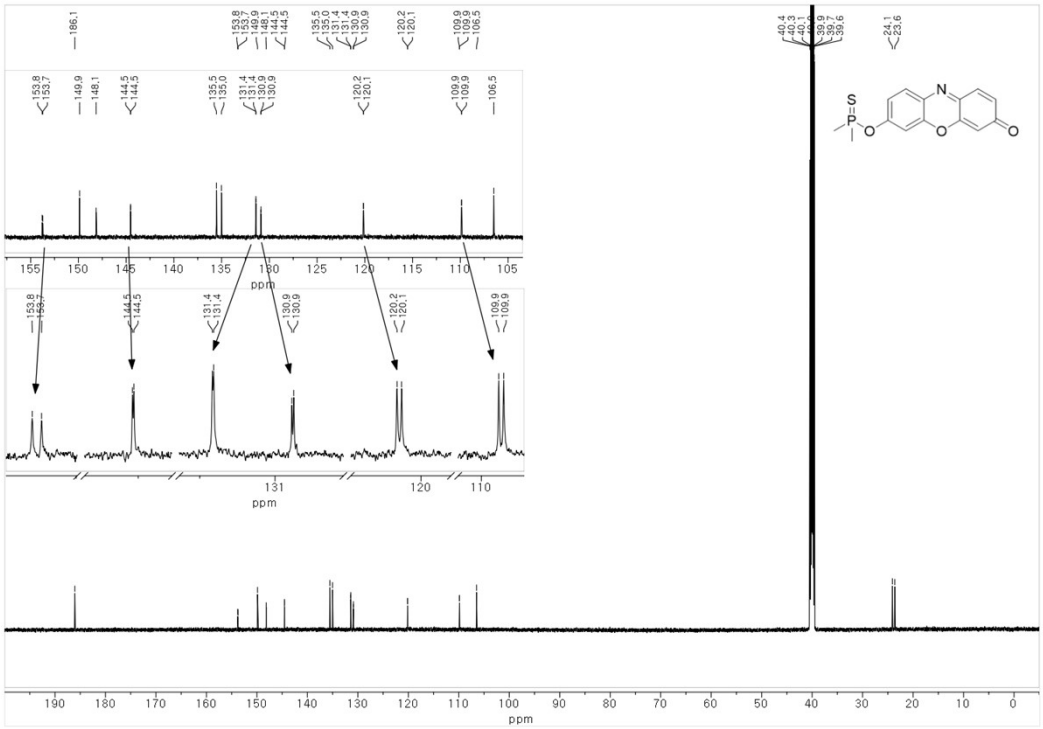

Fig. S14. ^{13}C NMR spectrum of **MP-1** in DMSO-d_6 (150 MHz).

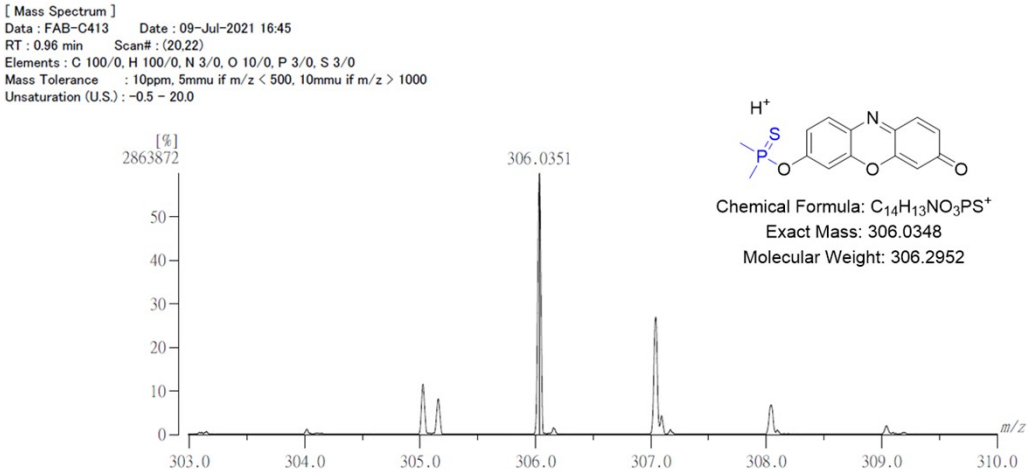

	Observed m/z	Int%	Err[ppm / mmu]	U.S.	Composition
1	306.0351	59.85	+15.5 / +4.7	19.5	C19 H4 N3 O2
2			+11.1 / +3.4	19.0	C21 H6 O3
3			-3.7 / -1.1	10.5	C12 H8 N3 O7
4			-8.1 / -2.5	10.0	C14 H10 O8
5			+5.1 / +1.6	6.0	C9 H10 N2 O10
6			+1.4 / +0.4	20.0	C20 H7 N2 P
7			+10.1 / +3.1	15.5	C17 H9 N O3 P
8			-9.1 / -2.8	6.5	C10 H13 N O8 P
9			+4.1 / +1.2	2.5	C5 H13 N3 O10 P
10			+0.3 / +0.1	16.5	C16 H10 N3 P2
11			-4.1 / -1.2	16.0	C18 H12 O P2
12			+9.1 / +2.8	12.0	C13 H12 N2 O3 P2
13			-10.1 / -3.1	3.0	C6 H16 N2 O8 P2
14			-5.1 / -1.6	12.5	C14 H15 N O P3
15			+8.1 / +2.5	8.5	C9 H15 N3 O3 P3
16			+3.7 / +1.1	8.0	C11 H17 O4 P3
17			-11.1 / -3.4	-0.5	C2 H19 N3 O8 P3
18			-8.6 / -2.6	19.5	C21 H8 N S
19			+4.5 / +1.4	15.5	C16 H8 N3 O2 S
20			+0.1 / +0.0	15.0	C18 H10 O3 S
21			+13.3 / +4.1	11.0	C13 H10 N2 O5 S
22			-14.7 / -4.5	6.5	C9 H12 N3 O7 S
23			-5.9 / -1.8	2.0	C6 H14 N2 O10 S
24			-9.7 / -3.0	16.0	C17 H11 N2 P S
25			-0.9 / -0.3	11.5	C14 H13 N O3 P S

Fig. S15. High-resolution FAB mass spectrum of **MP-1.**

References.

S1. D. C. Harris, in *Quantitative Chemical Analysis*, 8th ed., Freeman, New York, 2010, pp. 103–105.

S2. A. Kumar, D. Kumar and M. Chhibber, *ChemistrySelect*, 2020, **5**, 13738–13747.

S3. M. Rana, M. Balcioglu, N. M. Robertson, M. S. Hizir, S. Yumakc and M. V. Yigit, *Chem. Sci.*, 2017, **8**, 1200–1208.

S4. S. Zhu, Y. Zhuo, H. Miao, D. Zhong and X. Yang, *Luminescence*, 2015, **30**, 631–636.

S5. J. He, H. Zhang, J. Zou, Y. Liu, J. Zhuang, Y. Xiao, B. Lei, *Biosens. Bioelectron.*, 2016, **79**, 531–535.

S6. P. Singh and P. Sharma, *J. Photochem. Photobiol. A-Chem.*, 2021, **408**, 113096.

S7. C. Li, Q. Niu, J. Wang, T. Wei, T. Li, J. Chen, X. Qin, Q. Yang, *Spectroc. Acta Pt. A-Molec. Biomolec. Spectr.*, 2020, **233**, 118208.

S8. H. Tan, Y. Zhang, Y. Chen, *Sens. Actuator B-Chem.*, 2011, **156**, 120–125.